

# Evolution of avalanche conducting states in electrorheological liquids

A. Bezryadin, R. M. Westervelt, and M. Tinkham

*Department of Physics and Division of Engineering and Applied Sciences,  
Harvard University, Cambridge, Massachusetts 02138*

(October 21, 1998)

## Abstract

Charge transport in electrorheological fluids is studied experimentally under strongly nonequilibrium conditions. By injecting an electrical current into a suspension of conducting nanoparticles we are able to initiate a process of self-organization which leads, in certain cases, to formation of a stable pattern which consists of continuous conducting chains of particles. The evolution of the dissipative state in such system is a complex process. It starts as an avalanche process characterized by nucleation, growth, and thermal destruction of such dissipative elements as continuous conducting chains of particles as well as electroconvective vortices. A power-law distribution of avalanche sizes and durations, observed at this stage of the evolution, indicates that the system is in a self-organized critical state. A sharp transition into an avalanche-free state with a stable pattern of conducting chains is observed when the power dissipated in the fluid reaches its maximum. We propose a simple evolution model which obeys the maximum power condition and also shows a power-law distribution of the avalanche sizes.

PACS numbers: 64.60.Lx, 83.80.Gv, 82.70.Kj, 05.70.Ln.

## I. INTRODUCTION

A breaking of translational or temporal symmetry often occurs if a homogeneous, spatially extended system is driven far from equilibrium. This results in pattern formation [1]. The patterns (sometimes called “dissipative structures”) accelerate the energy dissipation and the motion of the system towards equilibrium. Spatiotemporal disorder which occurs if the patterns vary in time and space can involve the chaotic evolution of an amplitude field [2,3], or it can be connected with the dynamics of defects [4]. Also, out-of-equilibrium driven systems with *threshold* dynamics exhibit a rich phenomenology, from synchronized behavior [5] to self-organized criticality (SOC) [6,7], when the long-range correlations are manifested as power-law distributions of avalanche sizes and lifetimes [8,9].

In this paper we study the evolution of dissipative structures in initially homogeneous electrorheological fluids [10] suddenly driven out of equilibrium by applying a strong electric field. The driving mechanism of the evolution is found to be a competition between the forces which attempt to order the system and the destructive influence of increased thermal fluctuations. The ordering

forces appear when the system is driven out of equilibrium. In our case it is the electric field which polarizes the particles and leads to dipole-dipole attraction between them. The ordering leads to an increase in the dissipation rate. The increasing rate of the dissipation and associated temperature rise have an opposite, destructive effect on the self-organized structures.

Our attention will be restricted only to systems with *limited* dissipation. They consist of two parts: an “adaptive” subsystem (the electrorheological fluid) and a “rigid” subsystem (in our experiments it is a plain resistor connected in series with the fluid). The rigid part imposes an absolute limit on the power dissipated in the fluid. As a consequence, there is a global nonlinear interaction between all dissipative elements of the forming dissipative structure. Two types of collective behavior which lead to an increase in the dissipation rate have been encountered. These are (i) the conducting chains [11] which appear due to the dipole-dipole attraction and (ii) convective flows of electrically charged volumes of the liquid (see the illustration in Fig.1). The degree of order is characterized by the electrical current, which we can accurately measure. The charging of nanoparticles and the associated *repulsion* between them competes with the dipole-dipole *attraction* and renders the chain formation less evident than in usual electrorheological liquids with zero conductivity [12] where the charging is not possible.

New findings/results presented in this article are the following: (i) Two qualitatively different current-carrying states are found in electrorheological liquids exposed to a strong electric field. A “scale-invariant” avalanche state (AS) appears at the beginning of the evolution. It resembles the SOC state observed previously in, for example, sandpiles [8] and is characterized by a power-law distribution of avalanche sizes and durations (even though there is no external flux-drive [13]). (ii) The AS can transform itself into a stable state (SS) with a visible pattern of strings of nanoparticles (Fig.2). (iii) This transformation (which can be considered as a pattern formation) takes place only if the power dissipated by the adaptive part (the fluid) reaches its maximum (imposed by the rigid part). (iv) We propose a simple evolution model which obeys the “maximum power” principle [14,15] and shows an avalanche state with a power-law distribution of sizes and durations.

## II. EXPERIMENTAL DETAILS

The sample configuration is depicted in Fig.1. It consists of a pair of stainless-steel parallel cylindrical electrodes, 0.7 mm in diameter, separated by a distance of 10 mm and immersed over 10 mm into an electrorheological fluid. The fluid consists of a dielectric solvent (toluene) with ultrasonically dispersed conducting carbon nanoparticles [16] available commercially [17]. The concentration of particles is  $\approx 0.02\text{mg/ml}$ , which is far below the percolation threshold. Consequently, the initial resistance between the electrodes is high ( $\sim 10^{12}\Omega$ ). At time  $t = 0$  a DC voltage  $V_0 = 100\text{V}$  is applied to the electrodes through a series resistor  $R_s$  (Fig.1). Then an evolution curve, current vs time,  $I(t)$ , is measured. In the following discussion we will distinguish between curves measured on the “same sample”, and on “different samples”. In the first case a series of  $I(t)$  curves is measured on the same hermetically closed bottle with electrodes and the fluid. To restore the homogeneity, the fluid is excited ultrasonically before each new  $I(t)$  measurement [18]. Measurements on different samples means that a new, freshly prepared suspension is used for each new sample.

### III. TRANSPORT MEASUREMENTS

Experimentally we find three main Evolution Scenarios. (i) ES1: The first measurement on a freshly prepared suspension shows a monotonic growth of the current with time, if the concentration of particles is high enough. An example of such behavior is given in Fig.3a, curve “A”. (ii) ES2: Next measurements on the same sample show much more complicated curves with three different stages. For example, the curve “B” in Fig.3 was measured on the same sample as curve “A” after the fluid was again homogenized ultrasonically. Curves “C” and “D” were taken one after the other on a different sample, using a much higher series resistor  $R_s$ . They also illustrate the scenario ES2. Three different stages observed in the ES2 case are described below. Stage 1: During the first few hundreds of seconds (or less) after the voltage is applied, the current is small and it does not grow considerably; Stage 2 (avalanche state, AS): strong fluctuations of the current (by a factor of  $\approx 100$  in some cases) appear; the averaged value of the current ( $\langle I \rangle$ ) gradually increases. Stage 3: The current rapidly increases to yet a higher level and the fluctuations disappear. Thereafter the current continues to grow very slowly and monotonically. This new stable state (SS), which is the final stage of the evolution, is characterized by a visible and stable pattern of entangled strings composed of carbon particles. Examples of such strings are visible on the four bottom pictures of Fig.2. (iii) ES3: After a few successive measurements on the same sample the system can not reach the stable state any more, but the first two evolution stages are the same. Examples of such evolution curves are shown in Fig.3b, curves “E” and “F”. These curves were taken after the curves “C” and “D”, on the same sample. The avalanche state in ES3 case lasts  $\sim 10^5 s$  and finally, instead of the transition to the stable state, the current slowly decreases to zero; the conducting state “dies”. This happens when most of the particles cluster and settle down. (iv) After many ( $\sim 10$ ) measurements, the same sample shows no current growth at all.

The described evolution scenarios are quite general. They have been observed in liquids with different viscosity (toluene, hexadecane, mineral oil), with different electrodes (e.g. Pt, Sn), and at different values of the series resistors  $R_s$ . We have also found that the evolution scenarios described above can be observed not only by doing repetitive  $I(t)$  measurements on the same sample (this “aging” technique was described above) but also by reducing the concentration of the nanoparticles, while the  $I(t)$  curve is measured only once on each new sample with a freshly prepared suspension. The concentration reduction leads to the same transitions between evolution scenarios as the aging (when a series of  $I(t)$  measurements is made on the same sample). The aging approach was found to give much more reproducible results than the approach when the concentration is the control parameter.

### IV. IMAGING OF THE PATTERN FORMATION PROCESS

The evolution of patterns in electrorheological liquids can be observed directly with an optical microscope. Photographs shown in Fig.2 illustrate different stages for the evolution of the type ES2. The first image shows an aggregation process which takes place in the suspension of particles at zero electric field. Formation of fractal-like clusters is clearly visible.

The voltage was applied at time  $t = 0$  between the two electrodes (black). The applied field causes a strong polarization of the clusters (made of electrically conducting particles). The second photograph in Fig.2 shows that at  $t \approx 2 s$ , *i.e.* immediately after the voltage was applied, all big

aggregates break apart, so the fluid looks much more uniform. This rupture process is due to the polarization mentioned above. Since opposite sides of polarized clusters of nanoparticles carry opposite charges, big enough clusters are pulled apart if the applied electric field is strong enough.

During the first few hundreds of seconds the system shows some sort of collective behavior which may be called electroconvection or a “shuttling” effect. At this stage the electrical current is carried from one electrode to the other by macroscopic streams which develop in the fluid. Each stream carries many charged particles (or small clusters of particles) with the same charge. Upon the contact with the oppositely charged electrode, the particles acquire the opposite charge and start to move toward the opposite electrode. Initially those streams are very unstable and the flow looks “turbulent”. With time, new streams nucleate, become stronger and disappear. This shuttling effect is shown schematically in Fig.1. At this stage no stable strings were observed.

As time passes, the streams become bigger and slower. At some moment we observe an abrupt “stabilization” transition (which takes less than a second) when the turbulent electroconvection disappears and continuous strings of particles, extended from one electrode to the other, become visible. This is illustrated in Fig.2 (third image) which is taken a few seconds after the first stable strings became visible. Note that though we do not see the strings before the stabilization transition, we can not exclude that some strings of particles are being formed for a short time and then destroyed by heating or convection. After the pattern is stabilized, the strings show a tendency to form bundles. As is shown in the forth, fifth, and sixth images of Fig.2, these bundles grow continuously with time (which leads to the measured monotonic decrease of the sample resistance).

## V. THE MAXIMUM POWER PRINCIPLE

The electrical scheme of our setup is shown in Fig.1. The power dissipated by the electro-rheological fluid can be written as  $P_f = I(V_0 - V_s) = 4P_{max}/(r + 2 + 1/r)$  where  $P_{max} \equiv V_0^2/4R_s$ ,  $r \equiv R_f/R_s$ ,  $R_f \equiv V_f/I$  is the time-dependent resistance of the fluid,  $V_0$  is the battery voltage applied to the fluid and the resistor  $R_s$  connected in series (see the schematic in Fig.1),  $V_s$  ( $V_f$ ) is the voltage drop on the series resistor (fluid), and therefore  $V_0 = V_s + V_f$ . The expression for the  $P_f$  has a single maximum which is achieved when  $r = 1$  or  $R_f = R_s$ . Therefore the maximum power which can be dissipated by the fluid is  $P_{max} = V_0^2/4R_s$ . Note also that the expression for the  $P_f$  is symmetric under substitution  $r \rightarrow 1/r$  or, what is the same,  $R_f \rightarrow R_s^2/R_f$ . In other words, any allowed ( $P_f \leq P_{max}$ ) level of the dissipated power  $P_f$  (except only one point  $P_f = P_{max}$ ) can be achieved in two physically different states of the fluid. Our measurements show that these two states are qualitatively different. All states with  $R_f > R_s$  are characterized by strong avalanche-like current fluctuations. As soon as the fluid resistance decreases to the level  $R_f = R_s$  where dissipated power reaches its absolute maximum, the fluctuations disappear abruptly. At  $R_f < R_s$  the fluid resistance continues to decrease but slowly and monotonically. In Fig.4 we plot the power dissipated by the fluid (normalized by  $P_{max}$ ) versus time. Curves “G” and “I” (which correspond to the ES2 scenario) illustrate the maximum power principle for two different values of the series resistance  $R_s = 48.1M\Omega$  (curve “G”) and  $R_s = 1.04G\Omega$  (curve “I”). In both cases the huge current fluctuations disappear when the power reaches the maximum when  $P_f/P_{max} = 1$ . The curve “H” shows the normalized power vs time in the ES3 case. In this evolution scenario the power does not increase up to the  $P_f = P_{max}$  level. Consequently the system never stabilizes. To summarize, the experiment shows that the choice between the two scenarios (ES2 or ES3) is determined by

the ability of the adaptive part of the system with limited dissipation to reach the maximum rate of energy dissipation.

## VI. AVALANCHE STATE AND SELF-ORGANIZED CRITICALITY

It is interesting to compare the dynamics of fluctuations, observed in our systems, to the critical behavior of sandpiles and other self-organized systems. We suggest that the huge current fluctuations measured before the pattern is stabilized, constitute an avalanche activity of the dissipative structure. To make a quantitative comparison, we analyze the distribution of avalanche sizes ( $X$ ) defined as the amplitude (in Amperes) of each monotonic decrease of the current. This definition is acceptable since the noise level of our apparatus ( $< 1 \text{ pA}$ ) is much lower than the amplitude of the current fluctuations. Similarly, the duration of an avalanche  $T$  is defined as the duration (measured in seconds) of each monotonic current drop.

Statistical analysis shows that the avalanche activity in our system is scale invariant. This means that the avalanche distributions do not peak at any particular value. In the example of Fig.5b (see triangles), the avalanche-size probability density  $D_X$  follows a power-law distribution  $D_X \sim X^{-\alpha}$  (with  $\alpha \approx 1$ ) over about four decades. This suggests that the dissipative structure (before it is stabilized) is in the self-organized critical state. To corroborate this, we have found the distribution  $D_T$  of avalanche durations which is plotted in Fig.5c. It is also a power-law distribution:  $D_T \sim T^{-\beta}$ , as can be expected for a self-organized critical state. The exponent is larger in this case: ( $\beta \approx 2.3$ ). Other samples have shown a very similar behavior.

The distributions of avalanche sizes and durations, presented above, have been calculated for the evolution curves of the type ES3. In this cases the avalanche state lasts up to  $10^5 \text{ s}$ . In the ES2 case, the avalanche state lasts for a much shorter period of time, but the distributions are similar to those in the ES3 case.

## VII. DISSIPATIVE ELEMENTS AS BUILDING BLOCKS OF THE DISSIPATIVE STRUCTURE

Many properties of the pattern evolution, described above, can be understood by introducing the notion of “dissipative elements” (DE). The dissipative structure is assumed to be composed of relatively independent dissipative elements. In general, a DE is a region of space where any sort of self-organization or collective behavior (in our system it may be chain formation or electroconvection) leads to a strong increase of the local dissipation. The capability of each DE to dissipate energy  $G_i$  (which is electrical conductance in our case) as well as the total number of DE’s are assumed to grow with time. This reflects the general tendency of ordering, observed in nonequilibrium systems. This tendency will force more and more particles to join the existing dissipative elements or to form new ones. This process of ordering may be limited by the heating associated with the activity of each DE. To build a simple evolution model (see below) we will assume that any DE burns out when the power dissipated in it reaches some critical value  $P_c$ . This constitutes the threshold dynamics of our system.

Under the assumptions, outlined above, the evolution consists of nucleation, growth, and destruction of dissipative elements. The stabilization transition, observed experimentally, can be understood in the following way. In the case when the total rate of the dissipation is limited (by

the presence of a series resistor in our case), the pattern stabilizes if a sufficiently big number of DE's with high enough  $G_i$  values develops at the same time. In this case the total dissipated power (which is never bigger than  $P_{max}$ ) will be shared between a big number of DE's. Therefore the dissipation in each DE ( $P_i$ ) can never become strong enough for it to burn out.

It has to be explained why the stabilization coincides with the point of maximum power and does not depend on the properties of the fluid. This follows from the fact that  $P_f = 4P_{max}/(r + 2 + 1/r)$  and therefore the decreasing resistance (or increasing conductance) of the fluid causes an increase in the dissipation rate *only* if  $r > 1$  or  $R_f > R_s$ . Oppositely, if  $R_f < R_s$  then the increasing degree of order and associated decrease in the fluid resistance lead to a *decrease* in the power dissipated in the fluid. Therefore the pattern stabilizes as soon as the power reaches the maximum. We assume here that the degree of order always increases with time if the system is driven far enough from the equilibrium (meaning in our cases that the applied voltage is strong enough). Also we assume that the ordered structures may be destroyed due to the heating, but *only* if the local power reaches some critical value (as was already explained above).

### VIII. EVOLUTION MODEL

To confirm our hypothesis that the experimentally observed behavior is caused by nucleation, growth and destruction of DEs by the local heating associated with each DE, we suggest the following simple evolution model formulated in terms of electrical circuits. Let  $R_i$  to be electrical resistance of the  $i^{th}$  dissipative element. The conductance  $G_i = 1/R_i$  represents the efficiency of the  $i^{th}$  DE to dissipate energy. The number of particles joining each DE increases with time and so  $G_i$  increases as well. All DEs are assumed to be connected in parallel. We consider a model where the power dissipated by all DEs together can not exceed some value  $P_{max}$ . In the model (as well as in the experiment) the power is limited by a resistor  $R_s$  connected in series with DEs. The total current can be written as  $I = V_0/(R_s + 1/G_f)$  where the total conductance of the fluid is  $G_f = \sum_{i=1}^N G_i$ . The sum is taken over all available dissipative elements. Their total number will be  $N$  ( $N \gg 1$ ), but some of them may be switched off (meaning that  $G_i = 0$  for them). The “threshold dynamics” appears due to the assumption that the heating destroys the order in the  $i^{th}$  dissipative element and its conductance goes to zero if the power  $P_i = V_f^2 G_i$  dissipated by this particular DE exceeds some critical value  $P_c$  ( $P_c \ll P_{max}$ ). Since all DE's are assumed to be connected in parallel, they all will be biased with the same voltage  $V_f = V_0 - IR_s$  which depends on the total conductance of the fluid ( $G_f = 1/R_f$ ). Clearly this causes a global (and nonlinear) interaction between all DEs. Indeed, if one of the DEs burns out, then  $V_f$  increases and therefore some other DEs with a high conductance may burn out as well. This leads to further increase of the voltage  $V_f$  applied to the electrodes and may lead to destruction of other DE's. Such a “chain reaction” can explain the avalanches observed experimentally.

Our numerical model works as follows. At  $t=0$  all dissipative elements have zero conductance ( $G_i = 0$ ). Each time step we choose randomly  $N_1$  integer numbers  $K_m$  such that  $1 \leq K_m \leq N$ . Some of  $K_m$  numbers may be identical. Here  $N_1$  is a fixed number, such that  $1 \leq N_1 \leq N$ . It controls the nucleation rate of dissipative elements. The  $K_m$  numbers represent dissipative elements the conductance of which is going to be increased during the time step. The conductance of DEs with corresponding numbers  $K_m$  is increased in the following way:  $G_{K_m} \rightarrow G_{K_m} + RND$ . Here  $RND$  is a random value, such that  $0 < RND < STEP$ , and  $STEP$  is a constant representing the growth rate of DEs. Therefore the growth of each DE is a “biased random walk“. If two

numbers  $K_m$  are equal then  $G_{K_m}$  will be increased twice, and so on. After the conductance of all randomly chosen DE's is increased, following the algorithm explained above, we calculate the power dissipated in each DE using the expression  $P_i = V_f^2 G_i$ . If a dissipative element for which  $P_i > P_c$  is found, its conductance is put to zero, representing the destruction of this DE. After each such destruction event the voltage  $V_f$ , which is the same for all DE's, is updated. We proceed to the next time step only when there are no DE's with  $P_i > P_c$  left.

It is remarkable that this simple model can produce evolution curves which are very similar to the experimental ones. Three examples of the power versus time dependence are shown in Fig.6. In all these examples the DE nucleation rate  $N_1 = 5$  and the critical power  $P_c = 1.8P_{max}/N$  are the same. The parameter which is changed is the DE growth rate  $STEP$ . If the growth rate is low enough, the model generates a smooth evolution curve without avalanches, which look similar to the experimental curves of the type *ES1*. Such an example is given in Fig.6a. The absence of the avalanche activity is due to the low rate of the conductance growth, which means that a large number of DE's can form before any particular DE reaches its critical power point. So the total dissipated power can reach the maximum before any DE burns out. After the total power reaches its maximum, no dissipative elements will be destroyed because the probability that the rate of the heat dissipation in each particular DE would increase goes to zero.

At higher growth rates (see Fig.6b) the model generates more complicated evolution curves. Now it shows the transition from an avalanche to the stable state, similar to the experimentally measured *ES2* scenario. If the growth rate is chosen to be yet higher (Fig.6c), the normalized power ( $P_f/P_{max}$ ) always stays well below unity. Since it never reaches the maximum ( $P_f/P_{max} = 1$ ), the stabilization can not be achieved. Consequently the curve shown in Fig.6c represents the *ES3* scenario when the avalanche state lasts indefinitely long.

In the framework of our model, the same three types of behavior (*ES1*, *ES2*, and *ES3*) can be observed if the growth rate is kept constant while other parameters are changed. For example, at low values of the critical power we always observe the *ES3* scenario. By increasing the normalized critical power  $NP_c/P_{max}$  it is possible to shift the system to the *ES2* and even to the *ES1* scenario at yet higher values of the normalized critical power. The maximum power principle is always obeyed: The stabilization takes place only if the power can reach the absolute maximum. The model-generated evolution curves are also characterized by a power-law distribution of avalanche sizes (see Fig.5b, solid dots). The power-law exponent  $\alpha_{model} \approx 2$  is higher than the experimental value ( $\alpha \approx 1$ ). In many systems described previously by other authors an opposite relation was observed when the theoretically predicted value for the exponent  $\alpha$  was smaller than the values observed in experiments.

The model suggests three main parameters which control the transitions between different evolution scenarios. These parameters are the rates of nucleation and growth of dissipative elements and the normalized critical power  $NP_c/P_{max}$  of the DE's destruction. Experimentally we observe different evolution scenarios by aging the sample (see the discussion above). It is not well established which one of the control parameters changes during the aging. Preliminary observations suggest that in the process of the chain formation the particles can form stable clusters which can not be dissociated during subsequent ultrasonic excitation. This irreversible clustering leads to a decrease of the total number of independent particles participating in the chain formation, and consequently causes an effective decrease of the parameter  $N$  which represents the maximum number of chains. The normalized critical power  $NP_c/P_{max}$  decreases with decreasing  $N$ . This is one possible explanation for the aging process described in Section III which leads to the observed

transitions from ES1 to ES2 and subsequently to the ES3 type scenario.

Our model possesses certain similarities to the models developed by D. Sornette [13]. He proposed a class of models in which the self-organized nature of the criticality stems from the fact that the critical point (defined as the point when the coherence length becomes infinite:  $\xi \rightarrow +\infty$ ) is attracting the nonlinear feedback dynamics. His models are based on the existence of a feedback of the order parameter on the control parameter. Our model also possesses certain feedback mechanisms since the order parameter, say dissipated power, tends to destroy the order in the system. This leads to a decrease of the conductance and therefore causes a change of the voltage applied to the fluid, which can be considered as a control parameter. On the other hand our model is different since it is not spatially extended in the usual sense. In our model each dissipative element interacts with *all* other DE's with the same strength, not only with neighbor DE's. Therefore our model may be considered as a zero-dimensional one, so that the notion of critical state (which is used in Sornette's models) defined as the state when the coherence length diverges ( $\xi \rightarrow +\infty$ ), is not applicable to our system. Our model is based on an assumption that the order which develops in some *nonequilibrium* system may cause its own destruction due to the heat dissipated by the ordered structures themselves.

## IX. CONCLUSIONS

In conclusion, we present an experimental study of the evolution of patterns in a system with limited dissipation. Experiments are done on a new type of electrorheological fluid. A transition from the SOC-type scale-invariant avalanche state to a stable pattern is observed. It takes place when the power dissipated in the adaptive part of the system reaches its maximum defined by the rigid part. A general model of the pattern evolution in nonequilibrium systems with limited dissipation is suggested.

We thank D. Weitz and S. Maslov for useful discussions. This work was supported in part by NSF Grants DMR-94-00396, DMR-97-01487, and PHY-98-71810.

## REFERENCES

- [1] M. C. Cross and P. C. Hohenberg, Rev. Mod. Phys. **65**, 851 (1993).
- [2] J. Fineberg, E. Moses, and V. Steinberg, Phys. Rev. Lett. **61**, 838, (1988).
- [3] P. Kolodner, J. A. Glazier, and H. Williams, Phys. Rev. Lett. **65**, 1579 (1990).
- [4] A. La Porta and C. M. Surko, Phys. Rev. Lett. **77**, 2678 (1996).
- [5] S. H. Strogatz and I. Steward, Sci. Am. **269**, 102 (1993); A. V. M. Herz and J.J.Hopfield, Phys. Rev. Lett. **75**, 1222 (1995)
- [6] P. Bak, C. Tang, and K. Wiesenfeld, Phys. Rev. Lett. **59**, 381 (1987); H. Nakanishi, Phys.Rev.A, **41**, 7086 (1990).
- [7] Z. Olami, et al., Phys. Rev. Lett. **68**, 1244 (1992); Kwan-tai Leung et al., Phys. Rev. Lett. **80**, 1916 (1998).
- [8] G. A. Held, et al. Phys. Rev. Lett. **65**, 1120 (1990).
- [9] K. L. Babcock and R. M. Westervelt, Phys. Rev. Lett. **64**, 2168 (1990).
- [10] K. O. Havelka and F. E. Filisko, *Progress in Electrorheology* (Plenum Press, New York, 1995).
- [11] T. C. Halsey and W. Toor, Phys. Rev. Lett. **65**, 2820 (1990).
- [12] J. E. Martin and J. Odinek, Phys. Rev. Lett. **75**, 2827 (1995).
- [13] D. Sornette, J. Phys. I France **2**, 2065 (1992); D. Sornette, A. Johansen, and I. Dornic, J. Phys. I (France) **5**, 325 (1995).
- [14] H. T. Odum, Science, **242**, 1132 1988.
- [15] K. Nagel and M. Paczuski, Phys. Rev. E, **51**, 2909 (1995).
- [16] M.S. Dresselhaus, G. Dresselhaus, and P.C. Eklund, *Science of Fullerenes and Carbon Nanotubes* (Academic Press, New York, 1996), p.28-29.
- [17] Graphitized Carbon nanoparticles. The diameter is 27-30 nm. Polysciences Inc. (<http://www.polysciences.com>), cat.#08441.
- [18] Successive growths of chains followed by the ultrasonic mixing change properties of particles and let us observe all possible evolution scenarios without changing the particle concentration.

FIGURES

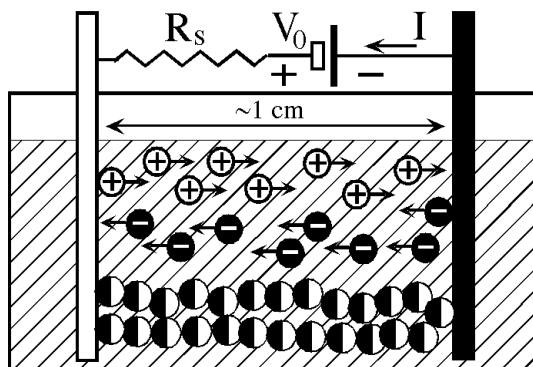


FIG.1 Schematic of the experimental setup. Two electrodes are immersed into electrorheological liquid (dashed region) and biased with  $V_0 = 100V$ . The charging of particles at the electrodes causes the electroconvection. Also, polarization of particles by the applied electric field leads to chain formation. The dissipated power is limited by the series resistor  $R_s$ .

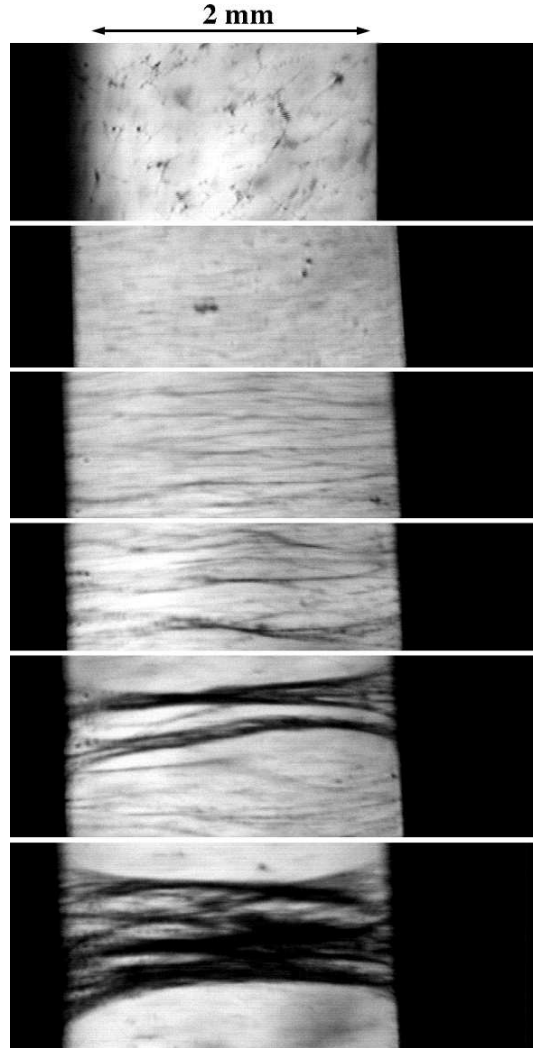


FIG.2 A time series of sample photographs, which illustrate the process of pattern formation. The electrodes are visible as black regions on the left and right sides of each image. The spacing between the electrodes is  $\approx 2mm$ . The first picture is taken before the voltage was applied ( $V = 0 V$ ,  $t < 0$ ). The following images show the process of pattern formation between the biased electrodes ( $V = 100 V$ ). They are take at  $t = 2, 300, 310, 350$ , and  $400$  seconds respectively. The third picture ( $t = 300 s$ ) is taken a few seconds after visible chains appeared for the first time. Subsequent photographs show the tendency of bundling.

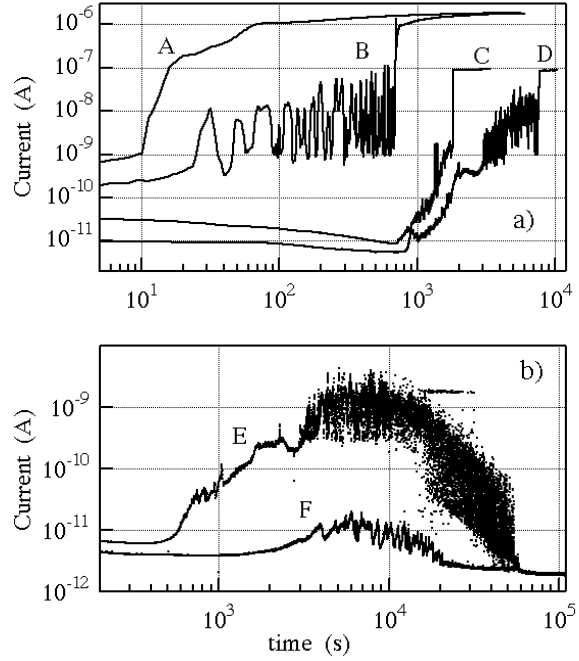


FIG.3 Examples of the evolution curves (current vs time) for two samples. (a) The curve B is measured after the curve A on the same sample with  $R_s = 48.1M\Omega$  and  $V_0 = 100V$ . Curves C, D, E, and F show successive runs on another sample with  $R_s = 1.04G\Omega$  and  $V_0 = 100V$  (curves E and F are plotted in the part (b)). The particle concentration was  $\approx 0.02mg/ml$  in all cases.

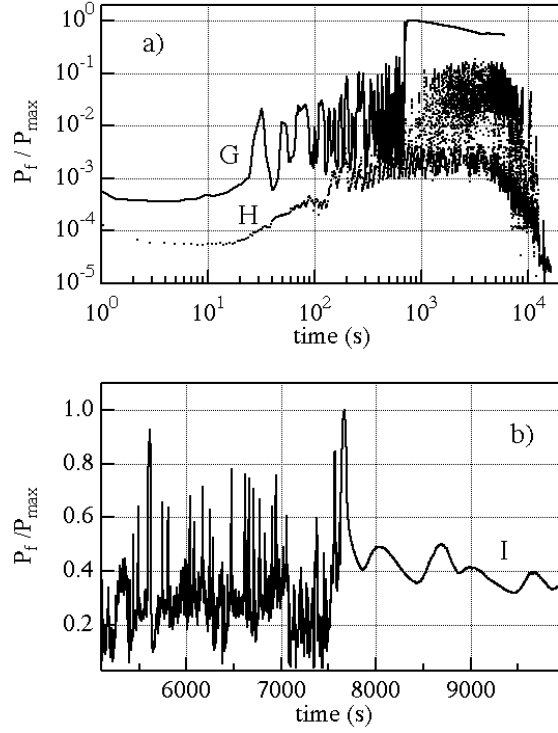


FIG.4 The total power dissipated by the fluid  $P_f = IV_f$ , normalized by the maximum power  $P_{max} = V_0^2/4R_s$ , is plotted vs time. The curves G and I are derived from curves B and D (Fig.3) respectively. The curve H is calculated from an  $I(t)$  curve measured after the curve B.

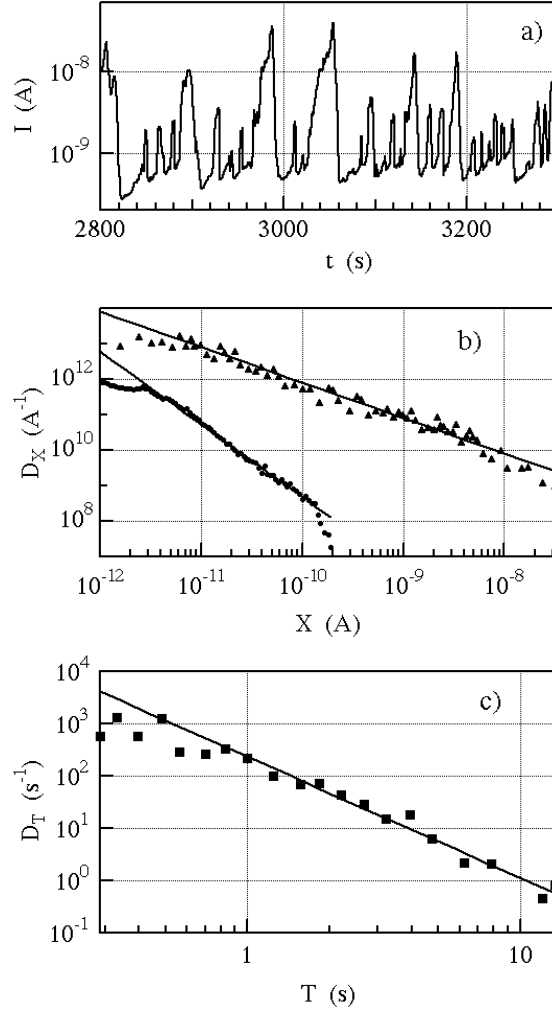


FIG.5 (a) A small segment of an evolution curve of the type ES3 measured at  $V_0 = 100V$  and  $R_s = 2.8M\Omega$ . (b) The top curve represents the distribution of avalanche sizes ( $X$ ) calculated from the experimental time dependence shown in (a). The straight line fit gives the probability density as  $D_X \sim X^{-\alpha}$  with  $\alpha = 1$ . The bottom curve shows a model-generated distribution of avalanche sizes. In this case the exponent in the power law is  $\alpha \approx 2$ . The bottom curve was shifted from its original position for clarity. (c) Distribution of avalanche durations ( $T$ ) found experimentally. The straight line is  $D_T \sim T^{-\beta}$ . The exponent of the power-law fit is  $\beta \approx 2.3$ .

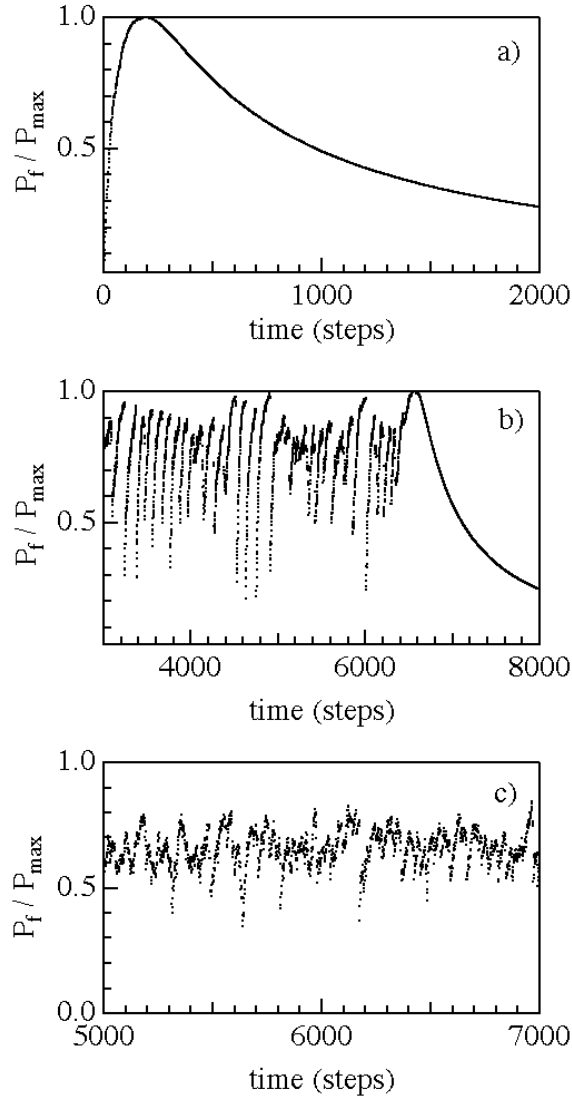


FIG.6 Three examples of model-generated evolution curves. All parameters are the same except the growth rate ( $STEP$ ) of the dissipative elements. This parameter has the value  $STEP = 0.2/NR_s$ ,  $0.3/NR_s$ , and  $0.6/NR_s$  for curves a), b), and c), respectively. The other parameters are  $N = 80$ ,  $N_1 = 5$ , and  $P_c = 1.8P_{max}/N$ .